Original Article

JCBFM

Journal of Cerebral Blood Flow & Metabolism
2019, Vol. 39(8) 1501–1515

DOI: 10.1177/0271678X18769515
journals.sagepub.com/home/jcbfm
SAGE

PDGFR-β restores blood-brain barrier functions in a mouse model of focal cerebral ischemia

Jie Shen[1,*], Guihua Xu[2,*], Runxiu Zhu[1], Jun Yuan[1], Yoko Ishii[3], Takeru Hamashima[3], Takako Matsushima[3], Seiji Yamamoto[3], Yusuke Takatsuru[4], Junichi Nabekura[5] and Masakiyo Sasahara[3]

Abstract

Although platelet-derived growth factor receptor beta (PDGFR-β) mediates the recruitment of vascular pericytes into ischemic lesion to restore the blood-brain barrier (BBB) dysfunction, its mechanisms still remain elusive. Compared with control *PDGFR-β*$^{floxed/floxed}$ mice (Floxed), postnatally induced systemic *PDGFR-β* knockout mice (Esr-KO) not only showed severe brain edema, neurologic functional deficits, decreased expression of tight junction (TJ) proteins, abundant endothelial transcytosis, and deformed TJs in the BBB, but also showed reduced expression of transforming growth factor-β (TGF-β) protein after photothrombotic middle cerebral artery occlusion (MCAO). In endothelial-pericyte co-culture, an *in vitro* model of BBB, the increment in the barrier function of endothelial monolayer induced by pericyte co-culture was completely cancelled by silencing *PDGFR-β* gene expression in pericytes, and was additively improved by PDGFR-β and TGF-β receptor signals under hypoxia condition. Exogenous PDGF-BB increased the expression of p-Smad2/3, while anti-TGF-β1 antibody at least partially inhibited the phosphorylation of Smad2/3 after PDGF-BB treatment *in vitro*. Furthermore, pre-administration of TGF-β1 partially alleviated edema formation, neurologic dysfunction, and TJs reduction in Esr-KO mice after MCAO. Accordingly, PDGFR-β signalling, *via* TGF-β signalling, may be crucial for restoration of BBB integrity after cerebral ischemia and therefore represents a novel potential therapeutic target.

Keywords

Blood-brain barrier, cerebral ischemia, pericyte, platelet-derived growth factor receptor-beta, transforming growth factor-β

Received 31 October 2017; Revised 13 February 2018; Accepted 14 March 2018

Introduction

The blood-brain barrier (BBB) plays a vital role in the homeostatic regulation of the brain microenvironment, and the disruption of BBB function is a contributing factor to brain injury in many diseases, including stroke.[1] Increased pinocytotic vesicles and the tight junction (TJ) protein derangement in endothelial cells contribute to BBB permeability after stroke, resulting in pericyte dysfunction, swollen astrocytic end-feet, and may contribute to cerebral vasogenic edema and haemorrhagic transformation.[1–3] Therefore, restoring BBB integrity is a promising therapeutic strategy for reducing the damage to the brain caused by ischemic stroke.

The platelet-derived growth factor (PDGF) family contains four ligands (A–D), which bind to two receptors (PDGFR-α and PDGFR-β).[4] PDGF-BB secreted

[1]Department of Neurology, Inner Mongolia Autonomous Region People's Hospital, Hohhot, Inner Mongolia, China
[2]Department of Clinical Medical Research Center, Inner Mongolia Autonomous Region People's Hospital, Hohhot, Inner Mongolia, China
[3]Department of Pathology, Graduate School of Medicine and Pharmaceutical Sciences, University of Toyama, Toyama, Japan
[4]Department of Integrative Physiology, Graduate School of Medicine, University of Gunma, Gunma, Japan
[5]Division of Homeostatic Development, National Institute for Physiological Sciences, Aichi, Japan
*These authors contributed equally to this work.

Corresponding authors:
Jie Shen, Department of Neurology, Inner Mongolia Autonomous Region People's Hospital, Zhaowuda Road 20, Hohhot 010010, Inner Mongolia, China.
Email: sj8017@163.com
Masakiyo Sasahara, Department of Pathology, Graduate School of Medicine and Pharmaceutical Sciences for Research, University of Toyama, 2630 Sugitani, Toyama 930-0152, Japan.
Email: sasahara@med.u-toyama.ac.jp

by endothelial cells binds to PDGFR-β on pericytes, causing the activation of downstream signalling pathways to regulate survival, migration, apoptosis, proliferation, and differentiation.[5] PDGF-BB/PDGFR-β signalling is essential for the pericytes-regulated BBB integrity in the stage of development,[6,7] and adulthood.[8] Furthermore, expression of PDGF-BB/PDGFR-β is upregulated in CNS after cerebral ischemia in human and animal models,[9–11] which is involved in tissue responses especially targeting vascular pericytes.[12] We have recently demonstrated that PDGFR-β signalling plays a vital role in BBB integrity and functional recovery after cerebral ischemia through the induction of pericyte recruitment, migration, and proliferation.[13] However, the underlying mechanisms of PDGFR-β signalling in pericyte-induced BBB restoration after cerebral ischemia is far from being fully understood.

The permeability of vascular endothelial cell monolayer *via* transcellular and paracellular pathways is tightly regulated by vesicular transport and tight junction (TJ) complex, respectively, and centrally comprises the barrier function of BBB. A number of molecular mechanisms are implied to regulate the BBB function, among which, PDGFR-β and transforming growth factor-β (TGF-β) may mediate the endothelial cell/pericyte interaction to protect the BBB integrity.[5] The brain pericyte-derived TGF-β strengthens the barrier function of an endothelial cell/pericytes co-culture model.[14] In a rat model of inflammatory pain, exogenous TGF-β1 can protect the integrity of BBB by enhancing TJ protein expression.[15] Thereafter, we investigated the mechanism of PDGFR-β signal-dependent restoration of BBB function after cerebral ischemia, focusing on the transcytosis and tight junction of vascular endothelial cells, as well as the involvement of TGF-β. For this end, we used postnatally induced systemic PDGFR-β knockout mice and an *in vitro* endothelial/pericyte co-culture model to examine the role of PDGFR-β and TGF-β signalling on BBB integrity after cerebral ischemia.

Materials and methods

All experimental animal procedures were conducted according to "the Institutional Animal Care and Use Committee at University of Toyama" (University of Toyama, 2630, Sugitani, Toyama city, 930-0194, Japan). All of our study protocols were approved by the Ethics Committee of University of Toyama. All studies followed the ARRIVE guidelines.

PDGFR-β conditional knockout mice

Mutant mice, in which exons 4–7 of PDGFR-β were flanked by two loxP sequences (PDGFR-$\beta^{floxed/floxed}$),[16] were cross-bred with chicken *β-actin*-promoter/*CMV*-enhancer-driven *Cre*-transgenic mice (*Cre-ER*$^{+/-}$; *CAGGCre-ER*$^{+/-}$; Jackson Laboratories, Bar Harbor, ME) that systemically expressed a fusion protein consisting of Cre recombinase and a mutated form of the mouse estrogen receptor ligand-binding domain.[17] The resulting male offspring expressing *PDGFR-*$\beta^{floxed/floxed}$*/Cre-ER*$^{+/-}$, and mice expressing *PDGFR-*$\beta^{floxed/floxed}$ were subjected to oral tamoxifen administration (9 mg/40 g body weight; five consecutive days; Sigma-Aldrich, Louis, MO, USA) at four weeks of age; the *PDGFR-*$\beta^{floxed/floxed}$*/Cre-ER*$^{+/-}$ mice were used as systematic PDGFR-β knockout mice (Esr-KO), and *PDGFR-*$\beta^{floxed/floxed}$ mice served as controls (Floxed), respectively. Mice were housed in an environment at 25°C, with a 12 h light/12 h dark cycle, and with *ad libitum* access to pelleted chow and water.

Focal cerebral ischemia

Mice were subjected to permanent MCAO as previously described.[18] The left middle cerebral artery (MCA) was exposed in five- to six-month-old male anesthetised mice (1–2% halothane/70% NO_2/30% O_2), while rectal temperature was maintained at 37 ± 0.5°C. Following intravenous administration of a photosensitizing rose bengal dye solution (20 mg/kg, Wako, Osaka, Japan), a 6-mW krypton laser operating at 568 nm (Melles Griot Inc, Tokyo, Japan) was used to irradiate the distal MCA for 4 min. After that, a secondary 4-min laser irradiation was administrated to the proximal MCA. The left common carotid artery (CCA) was then tightly ligated to induce a reproducible neocortical infarct.[19] The temporalis muscle and skin were subsequently reconstructed and the mice were subsequently maintained at a warm temperature and returned to the cage until resuscitation. Treatments were replicated on sham control mice, excluding the laser exposure and CCA ligation.

Measurement of brain edema

Absolute brain water content (ABWC) and edema formation were analysed as previously described.[20] Mice were decapitated under anaesthesia with sodium pentobarbital (50 mg/kg, Dainippon Sumitomo Pharma, Osaka, Japan) intraperitoneal injection, the brains were sagittally divided along the corpus callosum, and the contralateral and ipsilateral hemispheres were weighed immediately to obtain wet weight (WW). The tissue was dried to a constant weight at 50°C for 72 h and weighed to obtain dry weight (DW). The ABWC was calculated with the following formula: $\%H_2O = (WW\text{-}DW)/WW \times 100$. To analyse

the difference in ABWC between both hemispheres, the edema formation (%ΔH_2O) was calculated with the following formula: %ΔH_2O = %$H_2O_{ipsilateral}$ − %$H_2O_{contralateral}$.[20]

Haematoxylin-eosin (H-E) staining was performed to determine the space-occupying effect of the edema.[13] Under anaesthesia, mice were transcardially perfused with 0.01 M phosphate-buffered saline (PBS), followed by perfusion and immersion in 4% paraformaldehyde (PFA), after which the brains were embedded in paraffin overnight. Coronal sections (10 μm thick) were prepared with 200 μm intervals to cover the entire ischemic lesion. H-E staining was performed for the measurement of the areas of interest. Morphological and morphometrical analyses were performed using a microscopy system (BX 50; Olympus, Tokyo, Japan) connected to a digital camera (DP70; Olympus). Areas of interest were measured using MetaMorph software (Molecular Devices, Osaka, Japan). The space-occupying effect of edema was calculated with the following formula: (ipsilateral hemisphere volume − contralateral hemisphere volume)/ contralateral hemisphere volume.[20]

Measures of mouse behaviour

The corner turn test was performed before and after MCAO.[21] The test device consists of two vertical boards (each 30 cm × 20 cm × 1 cm) attached on one side at an angle of 30°. A food pellet in a small opening between the two boards encouraged the mice to enter the corner. Each mouse was placed at the entry of the corner facing to it. The mice rear on their hindlimbs and turned to the right or left side after reaching the corner, when both sides of the body (vibrissae, skin) were simultaneously stimulated. Turns were only recorded if mice fully rose on their hindlimbs. A total of 10 turns were counted with at least 30 s intervals between trials, and the percentage of right turns was calculated.

The adhesive removal test was performed before and after MCAO.[22] The mouse was placed at the centre of a transparent Perspex box ($48 \times 48 \times 30\,cm^3$, Melquest, Toyama, Japan) for a 60-s habituation period, and then two adhesive tapes ($0.3 \times 0.4\,cm^2$, 1010R, Nichiban Medical, Fukuoka, Japan) were applied with equal pressure on each mouse paw. The order of placement of the adhesive (right or left) was alternated between each animal and each session. The times to contact and to remove each adhesive tape were collected, with a maximum of 120 s. A five-day continuous training session (1 trial per day) was performed for each mouse before surgical procedures so that mice could reach optimal performances.

Western blot

For Western blot analysis, 2 mm thick coronal tissue sections were harvested from the centre of the ischemic lesions, as previously described.[13] The cortical ischemic lesion was dissected along the outer margin of the lesion and was designated as ipsilateral cortex. Cerebral cortex from a matching anatomical site was obtained from the unaffected hemisphere and was designated as contralateral cortex. After solubilizing the tissue, protein (15 μg) sample was separated by a 5–20% gradient gel (ATTO, Tokyo, Japan), followed by electroblotting onto polyvinylidene difluoride membranes (ATTO) and incubation in a blocking buffer of 5% non-fat milk at room temperature for 1 h. Membranes were incubated at 4°C overnight with the following primary antibodies: rabbit polyclonal anti-Claudin5 (1:500, Abcam, Cambridge, MA, USA), mouse monoclonal anti-Occludin (1:500, Invitrogen, Carlsbad, CA, USA), rabbit polyclonal anti-Zonula Occludens-1 (ZO-1, 1:500, Invitrogen), rabbit polyclonal anti-TGF-β (1:500, Abcam), rabbit polyclonal anti-angiopoietin 1 (Ang1, 1:500, Abcam), rabbit polyclonal anti-Tie2 (1:250, Santa Cruz Biotechnology, Santa Cruz, CA, USA), rabbit polyclonal anti-aquaporin4 (Aqp4, 1:200, Abcam), and mouse monoclonal anti-glyceraldehyde-3-phosphate dehydrogenase (GAPDH, 1:5000, Chemicon, Rosemont, IL, USA). The blots were incubated in horseradish peroxidase (HRP)-conjugated secondary antibody and developed using ECL plus Western blotting detection reagents (Amersham Biosciences, Little Chalfont, UK). The immunoreactive bands of targeted proteins were quantified by VH Analyzer software (VH-H1A5, Keyence, Osaka, Japan), and was normalised with the GAPDH protein band, and then relative to sham values.

Immunofluorescence staining in frozen tissue sections

Under deep anaesthesia, mice were transcardially perfused with ice-cold PBS, followed by perfusion 4% PFA. Frozen coronal sections (30 μm thick) were prepared, blocked, and stained using standard procedures.[23] Sections were incubated at 4°C overnight with the following primary antibodies: rabbit polyclonal anti-Claudin5 (1:100, Abcam), mouse monoclonal anti-Occludin (1:100, Invitrogen), rabbit polyclonal anti-ZO-1 (1:100, Invitrogen), and goat polyclonal anti-Glut1 (an endothelial cell marker, 1:100, Santa Cruz Biotechnology), mouse monoclonal anti-Aqp4 (1:100, Santa Cruz Biotechnology), rabbit polyclonal anti-glial fibrillary acidic protein (GFAP, 1:250, Dako), rabbit polyclonal anti-TGF-β (1:200, Abcam), and mouse monoclonal anti-Desmin (a marker of cerebrovascular pericytes, 1:200, Dako) in a blocking buffer of

10% normal donkey serum (Dako) at 4°C for two days. Secondary antibodies were raised in appropriate hosts and were conjugated with Alexa Fluor 488, Alexa Fluor 568 and Alexa Fluor 594 (1:500, Molecular Probes, Eugene, OR, USA). All sections were mounted with Vectashield mounting medium with 4′,6-diamidino-2-phenylindole (DAPI; Vector Laboratories, Burlingame, CA, USA) and were imaged with a confocal microscope (TCS-SP5, Leica). Montages were created using Photoshop software (version 7.0, Adobe, San Jose, CA, USA).

The areas of Glut1 positive blood vessels were determined within randomly-selected three squares of 0.16 mm^2 per section in the ischemic border, using a Biorevo BZ-9000 microscope (Keyence) and BZ-II Analyzer software (Keyence). The lengths of Claudin5, Occludin and ZO-1 positive staining were divided by the areas of Glut1 positive blood vessels. Three nonadjacent coronal sections per mouse were selected randomly and examined. Brain sections were selected from the same coronal level in sham-operated mice as from operated mice.

Transmission electron microscopy with horseradish peroxidase injection

Transmission electron microscopy analysis was performed after HRP injection according to the modified methods.[24,25] Under deep anaesthesia, mice suffered with MCAO were injected with HRP (type VI; 67 mg/kg, Sigma-Aldrich) solution intravenously. One hour after injection, mice were decapitated and the brain was trimmed into small tissue blocks ($<2 \times 2 \times 3\,mm^3$) in the outer margin of the ischemic lesion. The tissue blocks were fixed in 1% PFA fixative with 1.25% glutaraldehyde at 4°C overnight, cryoprotected in 30% sucrose in PBS until it sank, and then embedded in Tissue-Tek O.C.T. compound (Sakura Finetek). Vibratome sections of 60–100 μm thickness were prepared from these blocks, and rinsed overnight in 0.1 M phosphate buffer. The sections incubated in a medium containing 3,3′-diaminobenzidine tetrahydrochloride (DAB, Dako) and hydrogen peroxide (Dako) for 5 min were post-fixed in 2% osmium tetroxide (Sigma-Aldrich) for 2 h, dehydrated in ethanol, and then embedded in Epon 812 (TAAB Laboratories Equipment, Berkshire, UK) at 35°C for 24 h, 45°C for 24 h and 60°C for 48 h. Semi-thin sections of 1 μm thickness were cut from each block and stained with 1% toluidine blue (Sigma-Aldrich) to further trim the area of interest. After ultrathin sections of 60–80 μm thickness was cut with a diamond knife (Diatome, Biel, Switzerland) on a Reichert-Jung Ultracut E ultramicrotome (Leica), they were counterstained with uranyl acetate (Sigma-Aldrich) and lead citrate (Sigma-Aldrich), and observed with a JEM-1400TC electron microscope (JEOL, Tokyo, Japan). The number of HRP-labelled vesicles within vessels was determined per section in the ischemic border of the cerebral cortex. Three nonadjacent coronal sections per mouse were randomly selected and were examined. Brain sections from sham-operated mice were selected from the same coronal level as operated mice.

Intraventricular administration of TGF-β1

Human recombinant TGF-β1 was pre-administrated in the lateral ventricle of Floxed and Esr-KO mice at one day before MCAO according to the modified methods.[26] Briefly, under deep anaesthesia, a hole was made in the skull at the correct stereotaxic coordinates *via* a small dental drill, and then the dura matter was removed using small curved forceps. Using a microsyringe pump (CMA 400; Harvard Apparatus, Holliston, MA), TGF-β1 solution (1 ng/g, 1.5 μL, Sigma-Aldrich) was infused into the targeted location in the striatum at 1.0, 2.0, and 3.0 mm at anteroposterior relative to bregma, mediolateral, and dorsoventral from surface of the brain, respectively. The same amount of PBS was intraventricularly infused used as controls. At the sixth day after MCAO, edema formation and mouse behaviour were analysed, as described above. Protein (15 μg) samples were extracted from brain tissues, and then were used in Western blot analysis, as described above. Primary antibodies were used as follows: rabbit polyclonal anti-Claudin5 (1:500, Abcam), mouse monoclonal anti-Occludin (1:500, Invitrogen), rabbit polyclonal anti-Zonula Occludens-1 (ZO-1, 1:500, Invitrogen) and mouse monoclonal anti-GAPDH (1:5000, Chemicon). Samples was analysed in triplicate.

Cell culture and construction of in vitro BBB models

Human brain microvascular pericytes (HBMVPCs, ACBRI 499, Applied Cell Biology Research Institute, Kirkland, WA, USA) and human brain microvascular endothelial cells (HBMVECs, ACBRI 376, Applied Cell Biology Research Institute) were placed in uncoated culture flasks in CSC complete serum-free medium (SF-4Z0-500, Applied Cell Biology Research Institute) supplemented with 10% heat-inactivated fetal bovine serum (4Z0-500, Applied Cell Biology Research Institute), 100 units/ml penicillin, and 100 μg/ml streptomycin and incubated at 37°C with a humidified atmosphere of 5% CO_2/95% air. The cells were used for the generation of *in vitro* BBB models when reached 80–90% confluency.

To produce *in vitro* BBB models, HBMVPCs (1.5×10^4 cells/cm^2) were seeded onto the outside of the collagen-coated polycarbonate membrane

(1.12 cm^2, 0.4 μm pore size) of 12-well Transwell-Clear inserts (Costar, MA, USA) and directed upside down in the well of the 12-well culture plate (Costar), as previously described.[27] HBMVPCs were cultured for one day and then HBMVECs (1.5×10^5 cells/cm^2) were seeded on the inside of the insert placed in the well. The monolayer system consisted of HBMVECs alone. Culture medium (0.5 ml within the insert and 1.5 ml in the outer well) was replaced every other day. *In vitro* BBB models were constructed within three days after setting of HBMVECs.

siRNA transfection

HBMVPCs were transfected with *PDGFR-β* siRNA to inhibit *PDGFR-β* gene expression according to the manufacturer's instructions. Briefly, siRNA was diluted in Opti-MEM medium (51985042, Life Technologies, Carlsbad, CA, USA) and Lipofectamine™ 2000 transfection reagent (11668, Life Technologies) with a final concentration of 50 nM. The diluted siRNA mixture was incubated for 5 min at room temperature, and then added into the outer well of *in vitro* BBB models at 37°C for 48 h with a humidified atmosphere of 5% CO_2/95% air. To monitor siRNA transfection efficiency, *GAPDH* siRNA (AM4631, Life Technologies) transfection was used as a positive control. To test for nonspecific effects associated with siRNA delivery, Silencer® Negative control siRNA (AM4635, Life Technologies) transfection was used as a nonspecific negative control. Non-transfected BBB model was incubated with the same amount of diluted mixture without siRNA. The siRNA sequences are shown in Table 1. After siRNA transfection, *in vitro* BBB models were cultured under hypoxia condition (95% N_2/5% CO_2) at 37°C for 6 h, and then were used in the subsequent experiments.

Quantitative real-time polymerase chain reaction

Quantitative real-time PCR was performed as previously described.[13] Briefly, in co-culture systems, HBMVPs on the outside of the membrane were removed with a cell scraper. Total RNA was isolated using an RNeasy mini kit (Qiagen, Valencia, CA, USA), purified with an RNase-Free DNase Set (Qiagen, Valencia, CA, USA), and used as a template for cDNA synthesis by Prime Script RT reagent kit (Takara, Shiga, Japan). PCR reactions were performed in a Thermal Cycler Dice Real-Time System TP800 (Takara, Shiga, Japan) using SYBR Premix EX Taq (Takara, Shiga, Japan) according to the manufacturer's instructions as follows: 10 s at 95°C, 40 cycles of 5 s at 95°C, and 30 s at 60°C and then for the dissociation stage of 15 s at 95°C, 30 s at 60°C, and 15 s at 95°C. The primer sequences were as follows: *PDGFR-β*: forward primer, 5′-AGGACAACCGTACCTTGGGTG ACT-3′; reverse primer, 5′-CAGTTCTGACACGTA CCGGGTCTC-3′; *GAPDH*: forward primer, 5′-AA ATGGTGAAGGTCGGTGTG-3′; reverse primer, 5′-TGAAGGGGTCG TTGATGG-3′. Relative gene expression was determined by the standard curve method, and fold changes of targeted genes were normalised to *GAPDH* mRNA, relative to control values. Samples were analysed in triplicate.

MTT (3-(4,5-Dimethylthiazol-2-yl)-2,5-Diphenyl-Tetrazolium Bromide) assay

MTT assay was performed as previously described.[28] After 48 h of siRNA transfection, the MTT solution (Promega, 0.5 mg/ml) was added to HBMVPCs (2000 cells/well) seeded on 96-well and these were incubated for 1.5 h at 37°C. The same quantity of diluted mixture without siRNA was used as a vehicle. The amount of

Table 1. Primers of siRNAs and target genes.

Genes		Sequences
PDGFR-β siRNA-1 Start 2597	Sense 5′→ 3′	GGAUGAAUCUGUAGAUUAC
	Antisense 5′ → 3′	GUAAUCUACAGAUUCAUCC
PDGFR-β siRNA-2 Start 2687	Sense 5′ → 3′	CGAUAACUAUGUCCCAUCU
	Antisense 5′ → 3′	AGAUGGGACAUAGUUAUCG
PDGFR-β siRNA-3 Start 957	Sense 5′ → 3′	GUGGACUCCGAUACUUACU
	Antisense 5′→ 3′	AGUAAGUAUCGGAGUCCAC
GAPDH siRNA	Sense 5′ → 3′	CAGAAGACUGUGGAUGGCC
	Antisense 5′ → 3′	GGCCAUCCACAGUCUUCUG
Negative control	Sense 5′ → 3′	UUCUCCGAACGUGUCACGU
	Antisense 5′ → 3′	ACGUGACACGUUCGGAGAA

Note: Each experiment was performed at least three times. PDGFR-β: platelet-derived growth factor receptor-β; siRNA: small interfering RNA; GAPDH: glyceraldehyde-3-phosphate dehydrogenase.

formazan salt solubilised by acidic isopropanol (0.04 M hydroxychloride in absolute isopropanol) was measured by the absorbance at a wavelength of 570 nm. Samples were analysed in triplicate.

Terminal deoxyribonucleotide transferase-mediated dUTP nick-end labeling (TUNEL) staining

TUNEL staining was applied to siRNA-transfected HBMVPCs using a DeadEnd™ Fluorometric TUNEL System (Promega, Madison, WI, USA) according to the manufacturer's instructions. Briefly, after 48 h of siRNA transfection, HBMVPCs (2000 cells/well) seeded on 96-well were fixed in 4% paraformaldehyde at 4°C for 25 min, permeabilised in 0.2% Triton X-100 solution at room temperature for 5 min, and then incubated with the TUNEL reaction mixture at 37°C for 60 min in the dark. Wells were mounted with Vectashield mounting medium with DAPI and imaged with a confocal laser scanning microscope (TCS-SP5, Leica). Average percentage of TUNEL positive cells was calculated on randomly selected six fields of photograph from each Well.

TGF-β agonist and antagonist treatment

SB431542 (Sigma-Aldrich), a selective TGF-β type I receptor inhibitor was applied. After siRNA transfection, SB431542 solution (10 μM), which was dissolved in 100% dimethyl sulfoxide, was added into the outer well of *in vitro* BBB models under hypoxia condition (95% N_2/5% CO_2) at 37°C for 12 h. The same amount of dimethyl sulfoxide was used as black control. Human recombinant TGF-β1 (1 ng/ml, Sigma-Aldrich) was dissolved in 0.9% saline, and was added into the outer well of *in vitro* BBB models under hypoxia condition (95% N_2/5% CO_2) at 37°C for 12 h. The same amount of PBS was used as black control.

^{14}C-sucrose permeability

^{14}C-sucrose permeability was measured as previously shown.[29] After exposure to SB431542 or TGF-β1, the growth medium was replaced with assay buffer containing 122 mM NaCl, 25 mM $NaHCO_3$, 10 mM glucose, 3 mM KCl, 1.2 mM MgSO4, 0.4 mM K_2HPO_4, 1.4 mM $CaCl_2$ and 10 mM HEPES for 30 min at 37°C. Initially, 0.5 μCi of ^{14}C-sucrose (Sigma-Aldrich) was added to the inside of the insert (donor chamber). Immediately, 50 μl of solution was removed from the inside of the insert to determine the initial concentration of ^{14}C-sucrose. Samples (50 μl) were then collected from the outside of the insert (receiver chamber) at times 0, 30, 60, and 120 min, and an equal volume of fresh assay buffer was added at each time. The amount of radioactivity in each sample was measured in a liquid scintillation analyser (Tri-Carb 2100 TR, PerkinElmer Life Sciences, Boston, MA, USA). At least three inserts with cells and three inserts without cells were tested in each measurement, and each experiment was performed at least three times. The apparent permeability coefficient (PC_{app}) was calculated as $PC_{app}\ (cm/min) = (C_{R,\,t}/t \times V_R) / (C_D \times A)$ where $C_{R,\,t}$ is the concentration of ^{14}C-sucrose in receiver chamber at time t (mg/mL), V_R is the volume in the receiver chamber (1.5 ml), C_D is the initial concentration of ^{14}C-sucrose in the donor chamber (mg/mL) and A is the area of the membrane (1.12 cm^2). The final permeability coefficient (PC_f) was calculated as $1/PC_f = (1/PC_{app}) - (1/PC_m)$ where PC_m is the permeability coefficient of ^{14}C-sucrose across collagen-coated membrane without cells (mg/mL).

PDGF-BB stimulation assay

Exogenous PDGF-BB (40ng/ml, Sigma-Aldrich) was dissolved in 0.9% saline, and was added into the outer well of *in vitro* BBB models under hypoxia condition (95% N_2/5% CO_2) at 37°C for 12 h, with or without anti-TGF-β1 antibody (20μg/ml, Sigma-Aldrich) treatment for 1 h. Protein (15 μg) samples were extracted from post-treated pericytes in the outer well, and then were used in Western blot analysis, as described above. Primary antibodies were used as follows: rabbit polyclonal anti-p-Smad2/3 antibody (1:500, Abcam) and mouse monoclonal anti-GAPDH (1:5000, Chemicon). Samples were analysed in triplicate.

Statistics

Quantitative data were expressed as mean ± SEM. If data were normally distributed, comparisons between two experimental groups were made using unpaired Student's *t*-test. If the data, such as behavioural test and brain edema, were not normally distributed, analysis was done using non-parametric statistics and the Mann–Whitney U-test or Kruskal–Wallis test was used where appropriate. $P < 0.05$ was considered significant.

Results

In this study, we induced MCAO in 190 mice (Floxed, $n = 73$; Esr-KO, $n = 73$). Sham-operated mice were used as controls (Floxed, $n = 22$; Esr-KO, $n = 22$).

PDGFR-β deletion exacerbated edema formation and impaired functional recovery after cerebral ischemia

The three parameters including percentages of ABWC, edema formation, and space-occupying effect of edema

in the ipsilateral cerebral hemisphere were higher ($P < 0.01$) in Esr-KO mice than in Floxed mice at the six days after MCAO, but not at 3 or 14 days (Figure 1(a)). The corner turn test and adhesive removal test were conducted to evaluate long-term somatosensory and motor functions after focal cerebral ischemia. Before MCAO, all parameters were comparable between Floxed and Esr-KO mice (Figure 1(b) and (c)). Contralesional contact time, contralesional removal time and the percentage of right turns were increased ($P < 0.05$) in Esr-KO mice compared to Floxed mice from 3 to 14 days after MCAO (Figure 1(b) and (c)). Ipsilesional contact and removal times were comparable between two genotypes after MCAO (Figure 1(b) and (c)).

PDGFR-β deletion suppressed the recovery of tight junction proteins after cerebral ischemia

In the ipsilesional sides, protein levels of Claudin5 and Occludin were significantly decreased ($P < 0.05$ or $P < 0.01$) at 6 days after MCAO in Esr-KO mice compared to Floxed mice, respectively; while the ZO-1 levels were comparable between two genotypes through the experimental days (Figure 2(a)). In the contralesional sides, the expression levels of TJs were

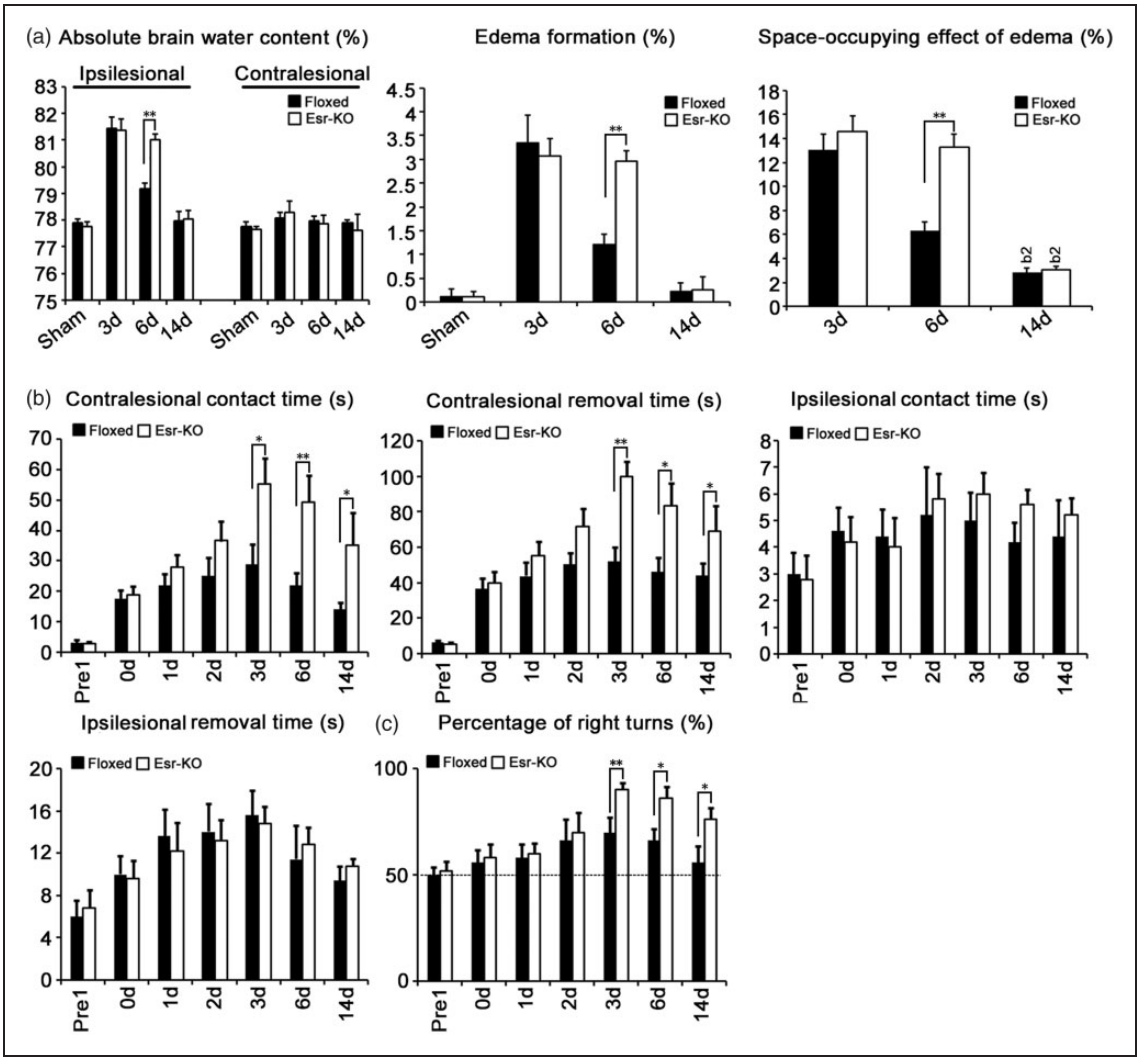

Figure 1. PDGFR-β deletion exacerbated edema formation and impaired functional recovery after cerebral ischemia. (a) Absolute brain water content, edema formation and space-occupying effect of edema in control mice (Floxed, $n = 7$) and PDGFR-β knockout mice (Esr-KO, $n = 7$) from 3 to 14 days after MCAO and sham-operated mice. (b) Adhesive removal test performances. Contralesional contact time and removal time, ipsilesional contact time and removal time in Floxed ($n = 7$) and Esr-KO ($n = 7$) mice before and after MCAO. (c) Percentage of right turns in Floxed ($n = 7$) and Esr-KO ($n = 7$) mice before and after MCAO. $^{*}P < 0.05$, $^{**}P < 0.01$.

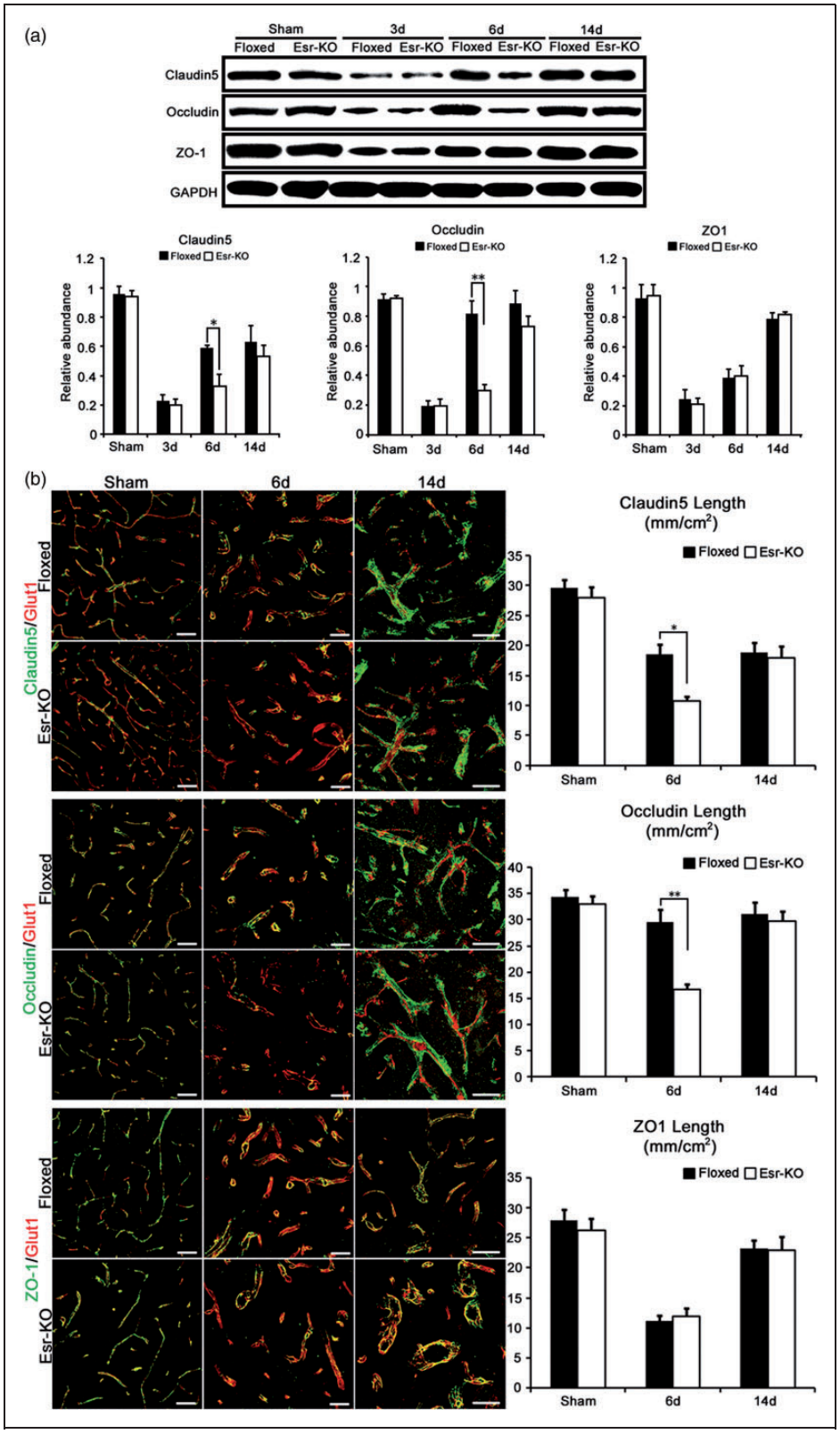

Figure 2. PDGFR-β deletion suppressed the recovery of tight junction proteins after cerebral ischemia. (a) Western blot analysis and quantification of Claudin5, Occludin, and ZO-1 protein expression in ipsilesional cerebral cortices of Floxed and Esr-KO mice after MCAO and sham-operated mice ($n = 3$ per group). Each bar was normalised by GAPDH. (b) Double-immunofluorescence staining for Claudin5 (green)/Glut1 (red), Occludin (green)/Glut1 (red) and ZO-1 (green)/Glut1 (red), and quantification of Claudin5, Occludin and ZO-1 length per area in the ischemic border of cerebral cortices of Floxed and Esr-KO mice at 6 and 14 days after MCAO and cerebral cortices of sham-operated mice (sham), $n = 6$ per group. Scale bars = 50 μm. *$P < 0.05$, **$P < 0.01$.

comparable between Floxed and Esr-KO mice ($P > 0.05$, data not shown).

In this line, immunohistochemistry showed that the proportions of blood vessels positive for Claudin5 and Occludin were significantly lower ($P < 0.05$ or $P < 0.01$) at six days after MCAO in Esr-KO mice compared to Floxed mice, respectively, whereas the proportion of ZO-1 positive blood vessels were comparable between two genotypes through the experimental days (Figure 2(b)). These three proteins were associating to the blood vessels at similar extents between two-genotypes and were not affected by MCAO in the contralateral side (data not shown).

PDGFR-β deletion increased transcellular transport and deformation of tight junctions after cerebral ischemia

Compared to Floxed mice, transmission electron microscopy analysis showed the significantly increased HRP-labelled vesicles ($P < 0.01$) and HRP accumulation in basal membrane in Esr-KO mice at six days after MCAO (Figure 3(a) c′, g′, i′, j′, k′), but not at 3 or 14 days.

The TJs are electron-dense linear structure along the interendothelial junctional cleft, and were of similar morphology between sham-operated Floxed and Esr-KO mice (Figure 3(b) a′, e′). These were identified as the structures of significant length along obliquely oriented stretch or vended form of interendothelial cleft in Floxed mice after MCAO (Figure 3(b) b′–d′). Comparing to them, interendothelial clefts were short with some gaps, and the associating electron-densities of TJs tended to be less intense in Esr-KO than in Floxed mice after stroke (Figure 3(b) f′–h′).

PDGFR-β deletion reduced expression of TGF-β protein after cerebral ischemia

To clarify the underlying mechanism of PDGFR-β signalling in BBB restoration, BBB integrity-related proteins (TGF-β, Ang1, Tie2 and Aqp4)[5,30] were tested in Western blot and immunohistochemical analyses. In the ipsilesional sides, protein levels of TGF-β were significantly decreased ($P < 0.05$ or $P < 0.01$) from 3 to 14 days after MCAO in Esr-KO mice compared to Floxed mice, respectively (Figure 4(a)), while there were no significant differences in the Ang1, Tie2, and Aqp4 protein levels between Floxed and Esr-KO mice in both ischemic lesion and contralateral hemisphere throughout the experimental period ($P > 0.05$, data not shown).

In the immunofluorescence analysis, TGF-β staining in Desmin-positive vascular cells was decreased in Esr-KO mice compared to Floxed mice at six days after MCAO (Figure 4(b)). Aqp4 positively stained cells closely surrounded blood vessels in the lesions, and were the proportion of these cells increased from 3 to 14 days in both Floxed and Esr-KO mice (Figure 4(c)). Cells stained positively for GFAP also closely surrounded blood vessels in the lesions, and were similarly increased from 3 to 14 days in both Floxed and Esr-KO mice (Figure 4(c)).

PDGFR-β signalling regulated BBB permeability via TGF-β in vitro and in vivo

As the above data imply that TGF-β may be a downstream mediator of PDGFR-β to induce BBB restoration after cerebral ischemia, we investigated the role of TGF-β and PDGFR-β in the barrier function of endothelial cell/pericyte co-culture that is a useful *in vitro* model of BBB. PDGFR-β expression in pericytes was supressed using PDGFR-β siRNA3, which effectively inhibited *PDGFR-β* mRNA to 14.9% ± 2.6% as compared with control siRNA (Figure 5(a)), but did not significantly affect the cell viability (Figure 5(b)), without induction of cellular apoptosis (Figure 5(c)).

TGF-β1 and the co-culture with pericytes individually, as well as additively improved the barrier function of endothelial cell monolayer ($P < 0.05$ or $P < 0.01$, Figure 5(d)). The increment of barrier function obtained after co-culture of two types of cells were completely cancelled by *PDGFR-β* gene suppression in pericytes, but this cancellation was again compensated by applied TGF-β1 ($P < 0.01$, Figure 5(d)). The TGF-β type I receptor inhibitor, SB431542, disturbed the barrier function of single endothelial cell monolayer as well as that of co-cultured cell layer ($P < 0.05$ or $P < 0.01$, Figure 5(d)). Furthermore, SB432542 disturbed the barrier function of co-cultured cell layer with inactivated *PDGFR-β* gene in pericytes ($P < 0.01$, Figure 5(d)). Exogenous PDGF-BB significantly increased the expression of p-Smad2/3, a downstream factor of TGF-β signalling pathway in pericytes ($P < 0.01$, Figure 5(e)), while anti-TGF-β1 antibody at least partially inhibited the phosphorylation of Smad2/3 after PDGF-BB treatment ($P < 0.05$, Figure 5(e)).

To further clarify the crosstalk between PDGFR-β and TGF-β signalling in the restoration of BBB integrity *in vivo*, TGF-β1 was pre-administrated in the lateral ventricle of Floxed and Esr-KO mice at one day before MCAO. Pre-administration of TGF-β1 significantly decreased edema formation, contralesional contact time and contralesional removal time in both Floxed and Esr-KO mice at six days after MCAO, compared with non-administration group, respectively ($P < 0.05$ or $P < 0.01$, Figure 5(f), (g)); moreover, the three parameters were less in Floxed than that in Esr-KO mice with pre-administration ($P < 0.05$ or $P < 0.01$,

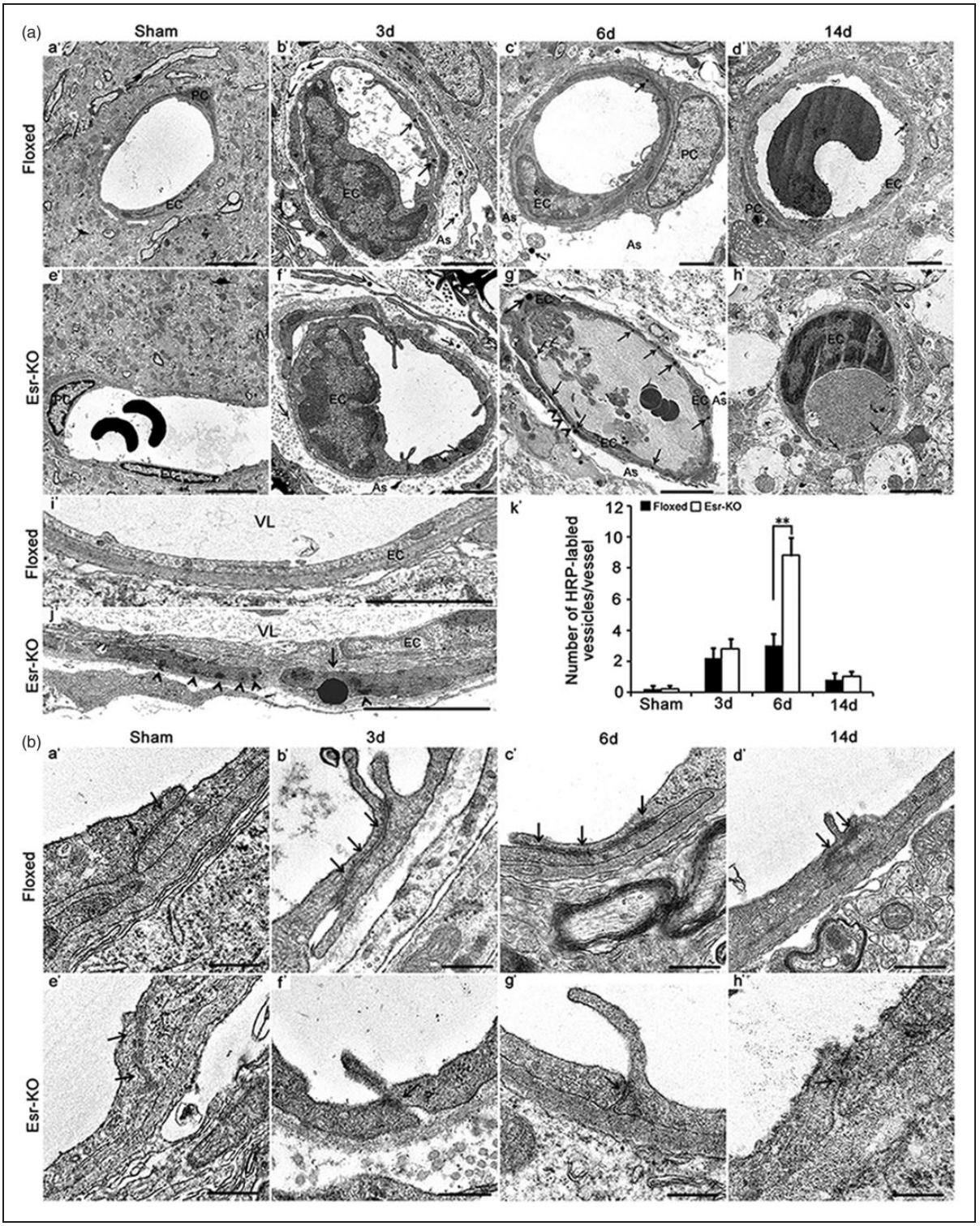

Figure 3. PDGFR-β deletion increased transcellular transport of deformation of tight junctions after cerebral ischemia. (a) Electron microscopy images and quantification of intravenously injected tracer-HRP labelled vesicles in the vascular endothelium in the ischemic border of Floxed and Esr-KO mice from 3 to 14 days after MCAO (b′–d′, f′–h′), and sham-operated mice (sham; $n = 6$ per group, a′, e′). (i′, j′): Electron microscopy images at higher magnification of intravenously injected tracer-HRP labelled vesicles in the vascular endothelium in the ischemic border of Floxed and Esr-KO mice at six days after MCAO. PC: pericyte, EC: endothelial cell; As: astrocyte; VL: vascular lumen; arrows indicate HRP-labelled vascular vesicles; arrowheads indicate HRP accumulation in basal membrane. Scale bars = 2 μm in Figure a′ to h′, 10 μm in (i′ and j′). (k′) Quantification of number of HRP-labelled vascular vesicles per vessel in the ischemic border of Floxed and Esr-KO mice from 3 to 14 days after MCAO and sham-operated mice (sham; $n = 6$ per group). $^{*}P < 0.05$, $^{**}P < 0.01$. (b) Deformation of tight junctions in the vascular endothelium in the ischemic border of Floxed and Esr-KO mice from 3 to 14 days after MCAO, and sham-operated mice (sham), $n = 6$ per group. Arrows indicate tight junctions. Scale bars = 400 nm.

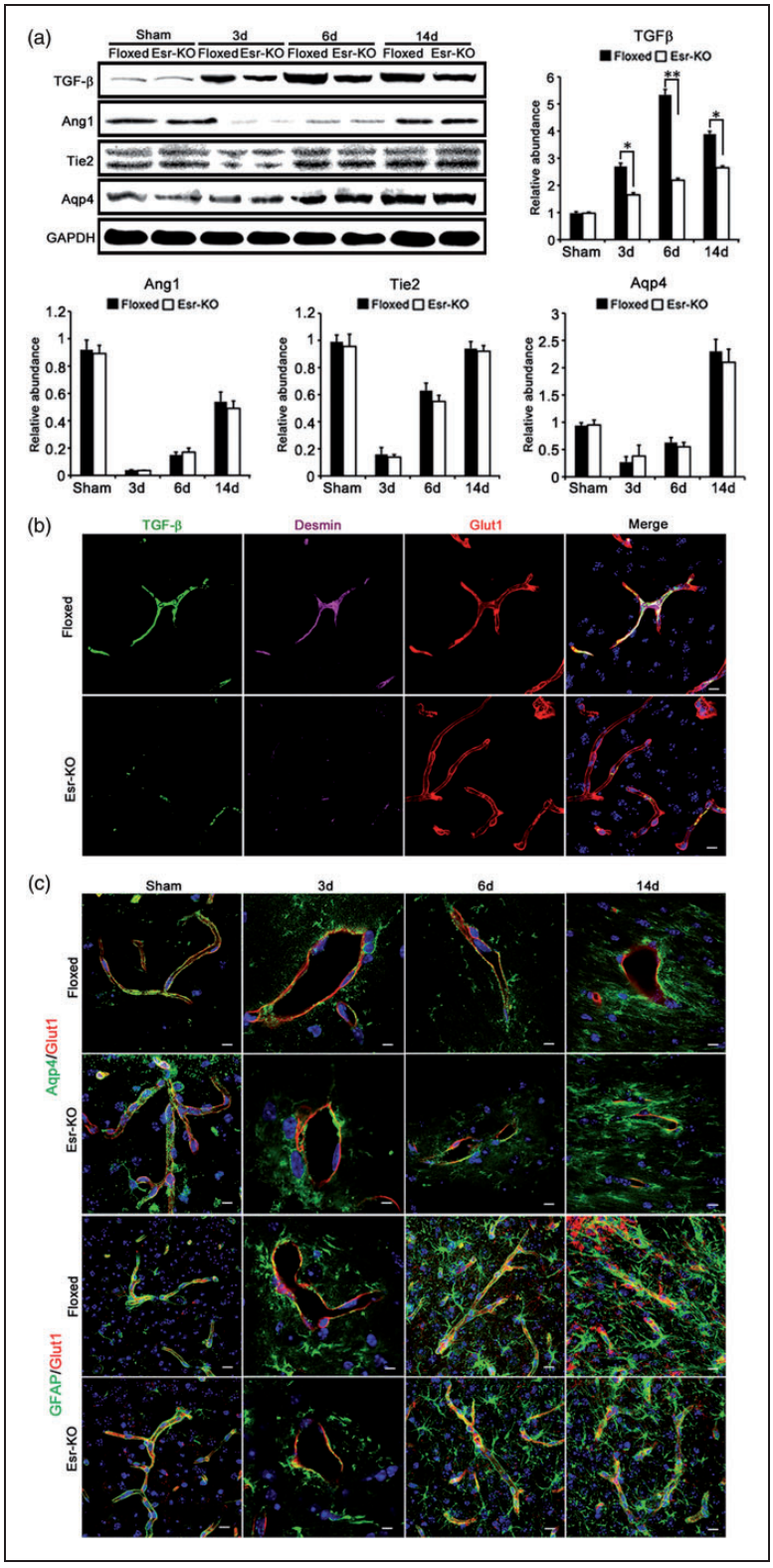

Figure 4. PDGFR-β deletion reduced expression of TGF-β protein after cerebral ischemia. (a) Western blot analysis and quantification of TGF-β, Angiopiontin 1(Ang 1), Tie2, Aquaporin 4 (Aqp 4) protein expressions in ipsilesional cerebral cortices of Floxed and Esr-KO mice after MCAO and sham-operated mice ($n = 3$ per group). Each bar was normalised by GAPDH. $^{*}P < 0.05$, $^{**}P < 0.01$. (b) Quadruple immunofluorescence staining for TGF-β (green)/Desmin (purple)/Glut1 (red) in the ischemic border of cerebral cortices of Floxed and Esr-KO mice at six days after MCAO. Counterstained with DAPI (blue). $n = 6$ per group. Scale bars = 10 μm. (c) Triple immunofluorescence staining for Aqp 4 (green)/Glut1 (red) and GFAP (green)/Glut1 (red) in the ischemic border of cerebral cortices of Floxed and Esr-KO mice at 6 and 14 days after MCAO and cerebral cortices of sham-operated mice (sham). Counterstained with DAPI (blue). $n = 6$ per group. Scale bars = 10 μm.

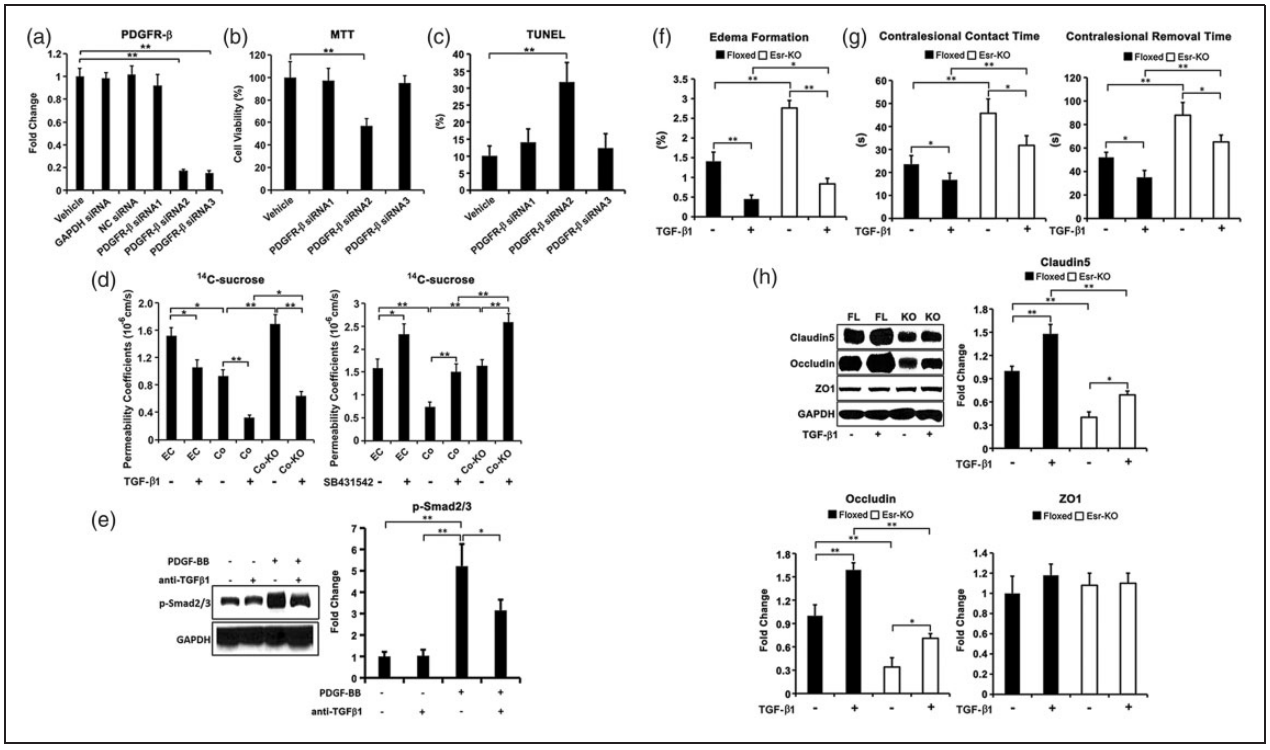

Figure 5. PDGFR-β signalling regulated BBB permeability *via* TGF-β *in vitro* and *in vivo*. (a) In *in vitro* co-culture model, quantitative real-time PCR of *PDGFR-β* mRNA with *GAPDH* siRNA, Negative control (NC) siRNA, three *PDGFR-β* siRNAs transfection or non-transfection (vehicle). (b) MTT assay and (c) TUNEL staining and percentage TUNEL-positive pericytes from *in vitro* co-culture model with three *PDGFR-β* siRNAs transfection or non-transfection (vehicle). (d) Exogenous TGF-β (1 ng/ml) treatment for permeability coefficients of ^{14}C-sucrose of HBMVECs alone (EC) and co-culture model (Co) and co-culture model with *PDGFR-β* siRNA knockdown (Co-KO), or no-treatment. SB431542 treatment (a selective TGF-β type I receptor inhibitor) for permeability coefficients of ^{14}C-sucrose of HBMVECs alone (EC) and co-culture model (Co) and co-culture model with *PDGFR-β* siRNA knockdown (Co-KO), or no-treatment. (e) Western blot analysis and quantification of p-Smad2/3 protein expression with PDGF-BB treatment and/or anti-TGF-β1 antibody treatment in co-culture model. (f) Edema formation, (g) contralesional contact time and removal time in control mice (Floxed, $n = 7$) and PDGFR-β knockout mice (Esr-KO, $n = 7$) at six days after MCAO with or without pre-administration of TGF-β1. (h) Western blot analysis and quantification of Claudin5, Occludin, and ZO1 protein expression in ipsilesional cerebral cortices of Floxed and Esr-KO mice ($n = 3$ per group) at 6 days after MCAO with or without pre-administration of TGF-β1. $^{*}P < 0.05$, $^{**}P < 0.01$.

Figure 5(f), (g)). Pre-administration of TGF-β1 significantly increased protein levels of Claudin5 and Occludin in both Floxed and Esr-KO mice at six days after MCAO, compared with non-administration group, respectively ($P < 0.05$ or $P < 0.01$, Figure 5(h)); moreover, the two protein levels were higher in Floxed than that in Esr-KO mice with pre-administration ($P < 0.01$, Figure 5(h)). Pre-administration of TGF-β1 did not modify protein level of ZO1, compared with the same genotypic non-administration group, respectively ($P > 0.05$, Figure 5(h)).

Discussion

The present study is the first to address the crosslink between PDGFR-β and TGF-β signalling in BBB integrity by regulating pericyte-induced expression of TJ proteins in response to ischemia/hypoxia both *in vitro* and *in vivo*.

In sham-operated or non-ischemic cerebral cortices of Esr-KO mice, expression of TJ proteins (Claudin5, Occludin and ZO-1) were well preserved in immunostaining and western blot. Furthermore, no significant change was found in ultrastructure of TJ and endothelial transcytosis in these regions, with undetectable edema formation. These findings were compatible with our previous report showing unchanged pericyte coverage and negligible FITC-albumin leakage in the same mouse model.[13] In contrast, congenital disturbance of the PDGF-B/PDGFR-β signalling axis resulted in pericyte loss and abnormal BBB leakage during the early developing period, which can potentially persist long till to adult.[6,7,31,32] These findings indicate that the PDGF-B/PDGFR-β signalling axis is essential for the

development/organogenesis, but not for the maintenance of pericytes and BBB function in the normal adult brain. The congenital deficits of PDGF-B/PDGFR-β signalling severely disturb the organogenesis of kidney glomerulus.[33] However, postnatal deletion of PDGFR-β does not adversely affect the structure and physiologic functions of the glomerulus.[34] This indicates that PDGF-C/PDGFR-α signalling is a potential candidate to compensate for the loss of PDGFR-β in adult cerebral pericytes, as PDGF-CC also activates PDGFR-α and promotes the proliferation, survival, and migration of retinal pericytes.[35]

In cerebral ischemia, PDGFR-β was found to be markedly increased specifically in peri-infarct pericytes, and partly contributing to pericyte growth and survival *via* Akt pathway.[36] Using *in vivo* angiogenesis and ischemic hind-limb animal models, PDGF-AB/FGF-2 has been demonstrated to be able to stabilise the newly formed vasculature by recruiting pericytes, and an anti-PDGFR-β neutralising antibody significantly blocks PDGF-AB/FGF-2-induced vessel stability.[37] In this line, the results of our previous study showed that in the ischemic Esr-KO lesion, the number of pericytes was severely decreased and BBB leakage was extensive, which was shown by the increased extravasation of fluorescent-labelled tracer. These phenotypes detected in Esr-KO mice were significantly rescued in neuroepithelium-derived PDGFR-β deficient mice, in which PDGFR-β expression was preserved in pericytes.[13] In the present study, PDGFR-β deficiency lead to severe edema formation, with impaired somatosensory and motor functions after MCAO. PDGFRβ+ pericytes have been previously shown to move toward injured areas to stabilise leaky blood vessels and initiate glial scar formation to seal the damaged areas after brain injury.[38] These indicate that PDGFR-β signalling is necessary for pericyte recruitment, BBB integrity, and functional recovery in the injured adult mouse brain.

The regulation of endothelial BBB tight and adherens junction protein expression, the alignment of TJ proteins, and bulk-flow transcytosis of fluid-filled vesicles across the BBB are all potential mechanisms through which cerebral pericytes contribute to BBB integrity.[5–8] In an *in vitro* BBB model, pericytes are more effective than astrocytes at inducing Claudin5 and ZO-1 expression, TJ proteins that regulates BBB permeability, and improving transendothelial electrical resistance values during prolonged oxygen deprivation.[39] Similarly, in the present study, Esr-KO mice showed TJ deformation and increased endothelial transcytosis in the ischemic lesion, which is concomitant with severe edema formation at 6 day after MCAO. However, further studies are needed to understand the mechanisms through which PDGFR-β signalling activates pericyte-induced BBB restoration after cerebral ischemia.

Our results showed that the expression of TGF-β protein in Esr-KO mice is significantly lower than in Floxed mice, particularly at six days after MCAO in the Western blot and immunofluorescence analysis, consistent with the edema formation and TJ deformation. Considering the crucial roles played by TGF-β signalling in cell differentiation, maturation, proliferation, migration, and attachment of pericytes,[5] the co-culture model was used to test the effects of treatment with exogenous TGF-β1 or SB431542, a selective TGF-β type I receptor inhibitor. Increased ^{14}C-sucrose permeability with *PDGFR-β* silencing in pericytes showed the deterioration in BBB integrity. In contrast, exogenous TGF-β1 exposure at least partly decreased ^{14}C-sucrose permeability, while SB431542 exacerbated the effect of *PDGFR-β* silencing. Furthermore, pre-administration of TGF-β1 partially alleviated edema formation, neurologic dysfunction, and TJs reduction in Esr-KO mice after MCAO. These confirmed the previous studies showing that pericyte-secreted TGF-β promotes BBB integrity *via* enhanced endothelial TJ expression *in vitro* and *in vivo*.[14,40] Deletion of TGF-β has been reported to result in pericyte coverage loss, tortuous vessels, endothelial hyperplasia and vessel haemorrhaging.[41] Moreover, exogenous PDGF-BB increased the expression of p-Smad2/3, while anti-TGF-β1 antibody at least partially inhibited the phosphorylation of Smad2/3 after PDGF-BB treatment *in vitro*, indicating that TGF-β may be a downstream effector of PDGFR-β. It is considered that the PDGF-BB/PDGFR-β signalling pathway is potentially involved in the BBB function by promoting pericyte proliferation and differentiation specifically *via* PI3K-PKC-TGF-β signalling.[5] Overall these data indicate that PDGFR-β signalling plays a pivotal role in BBB restoration after cerebral ischemia, in part *via* the regulation of TGF-β signalling. However, further studies will require more effective and dynamic strategies to fully understand the crosslink between two signalling.

It is worth to note that the infarction volume and worse functional outcomes after cerebral ischemia may be not solely due to disruption of BBB integrity relating to pericyte loss. Our findings still cannot rule out the other underlying mechanisms, as pericytes are multipotency and are able to differentiate into neural cells, vascular cells, and microglia in response to ischemia/hypoxia.[42,43] Based on that pericytes play several diverse roles during the distinct stages of ischemic stroke, further studies will require more effective and dynamic strategies to fully understand their roles.[44]

In conclusion, our findings indicate that enhancement of PDGFR-β signalling in pericytes can improve

BBB integrity, minimise brain edema, improve clinical outcomes, and may be a novel potential therapeutic target for ischemic stroke. Further experiments are needed to elucidate the regulatory role and synergistic mechanisms of PDGFR-β and TGF-β signalling on BBB integrity.

Funding

The author(s) disclosed receipt of the following financial support for the research, authorship, and/or publication of this article: This work was supported by the National Natural Science Foundation of China [grant numbers 81360186, 81460190], the Grants-in-Aid for Scientific Research from the Ministry of Education, Culture, Sports, Science and Technology of Japan, and Core Research for Evolutional Science and Technology, Japan Science and Technology Agency (CREST, JST) [grant numbers 20390108, 20590381, 24790378].

Acknowledgment

We thank Yoichi Kurashige (University of Toyama, Japan) for his technological assistance.

Declaration of conflicting interests

The author(s) declared no potential conflicts of interest with respect to the research, authorship, and/or publication of this article.

Authors' contributions

JS, GX, MS had access to all the data in the study and takes responsibility for the integrity of the data; MS, JS, GX and YI conceived and designed research; MS, JS, GX, RZ, JY, TH, TM, SY, YT, and JN contributed to data acquisition; JS, GX, YI and MS performed the data analysis and interpretation; JS, GX and MS wrote the manuscript. All authors revised and approved the final submission.

References

1. Prakash R and Carmichael ST. Blood-brain barrier breakdown and neovascularization processes after stroke and traumatic brain injury. *Curr Opin Neurol* 2015; 28: 556–564.
2. Zhao Z, Nelson AR, Betsholtz C, et al. Establishment and dysfunction of the blood-brain barrier. *Cell* 2015; 163: 1064–1078.
3. Cai W, Liu H, Zhao J, et al. Pericytes in brain injury and repair after ischemic stroke. *Transl Stroke Res* 2017; 8: 107–121.
4. Tallquist M and Kazlauskas A. PDGF signalling in cells and mice. *Cytokine Growth Factor Rev* 2004; 15: 205–213.
5. Sweeney MD, Ayyadurai S and Zlokovic BV. Pericytes of the neurovascular unit: key functions and signalling pathways. *Nat Neurosci* 2016; 19: 771–783.
6. Armulik A, Genove G, Mae M, et al. Pericytes regulate the blood-brain barrier. *Nature* 2010; 468: 557–561.
7. Daneman R, Zhou L, Kebede AA, et al. Pericytes are required for blood-brain barrier integrity during embryogenesis. *Nature* 2010; 468: 562–566.
8. Bell RD, Winkler EA, Sagare AP, et al. Pericytes control key neurovascular functions and neuronal phenotype in the adult brain and during brain aging. *Neuron* 2010; 68: 409–427.
9. Fernández-Klett F, Potas JR, Hilpert D, et al. Early loss of pericytes and perivascular stromal cell-induced scar formation after stroke. *J Cereb Blood Flow Metab* 2013; 33: 428–439.
10. Makihara N, Arimura K, Ago T, et al. Involvement of platelet-derived growth factor receptor β in fibrosis through extracellular matrix protein production after ischemic stroke. *Exp Neurol* 2015; 264: 127–134.
11. Sakuma R, Kawahara M, Nakano-Doi A, et al. Brain pericytes serve as microglia-generating multipotent vascular stem cells following ischemic stroke. *J Neuroinflammation* 2016; 13: 57.
12. Nakamura K, Arimura K, Nishimura A, et al. Possible involvement of basic FGF in the upregulation of PDGFRβ in pericytes after ischemic stroke. *Brain Res* 2016; 1630: 98–108.
13. Shen J, Ishii Y, Xu G, et al. PDGFR-β as a positive regulator of tissue repair in a mouse model of focal cerebral ischemia. *J Cereb Blood Flow Metab* 2012; 32: 353–367.
14. Dohgu S, Takata F, Yamauchi A, et al. Brain pericytes contribute to the induction and up-regulation of blood-brain barrier functions through transforming growth factor-beta production. *Brain Res* 2005; 1038: 208–215.
15. Ronaldson PT, Demarco KM, Sanchez-Covarrubias L, et al. Transforming growth factor-beta signalling alters substrate permeability and tight junction protein expression at the blood-brain barrier during inflammatory pain. *J Cereb Blood Flow Metab* 2009; 29: 1084–1098.
16. Gao Z, Sasaoka T, Fujimori T, et al. Deletion of the PDGFR-β gene affects key fibroblast functions important for wound healing. *J Biol Chem* 2005; 280: 9375–89.
17. Hayashi S and McMahon AP. Efficient recombination in diverse tissues by a tamoxifen-inducible form of Cre: a tool for temporally regulated gene activation/ inactivation in the mouse. *Dev Biol* 2002; 244: 305–18.
18. Sugimori H, Yao H, Ooboshi H, et al. Krypton laser-induced photothrombotic distal middle cerebral artery occlusion without craniectomy in mice. *Brain Res Brain Res Protoc* 2004; 13: 189–196.
19. Brint S, Jacewicz M, Kiessling M, et al. Focal brain ischemia in the rat: methods for reproducible neocortical infarction using tandem occlusion of the distal middle cerebral and ipsilateral common carotid arteries. *J Cereb Blood Flow Metab* 1988; 8: 474–485.
20. Gerriets T, Stolz E, Walberer M, et al. Noninvasive quantification of brain edema and the space-occupying effect in rat stroke models using magnetic resonance imaging. *Stroke* 2004; 35: 566–571.
21. Zhang L, Schallert T, Zhang ZG, et al. A test for detecting long-term sensorimotor dysfunction in the mouse after focal cerebral ischemia. *J Neurosci Meth* 2002; 117: 207–214.

22. Bouet V, Boulouard M, Toutain J, et al. The adhesive removal test: a sensitive method to assess sensorimotor deficits in mice. *Nat Protoc* 2009; 4: 1560–1564.
23. Yamashita S and Okada Y. Application of heat-induced antigen retrieval to aldehyde-fixed fresh frozen sections. *J Histochem Cytochem* 2005; 53: 1421–1432.
24. Ueno M, Akiguchi I, Hosokawa M, et al. Blood-brain barrier permeability in the periventricular areas of the normal mouse brain. *Acta Neuropathol* 2000; 99: 385–392.
25. Saadoun S, Tait MJ, Reza A, et al. AQP4 gene deletion in mice does not alter blood-brain barrier integrity or brain morphology. *Neuroscience* 2009; 161: 764–772.
26. Zheng Y, Yamamoto S, Ishii Y, et al. Glioma-derived platelet-derived growth factor-BB recruits oligodendrocyte progenitor cells via platelet-derived growth factor receptor-α and remodels cancer stroma. *Am J Pathol* 2016; 186: 1081–1091.
27. Nakagawa S, Deli MA, Nakao S, et al. Pericytes from brain microvessels strengthen the barrier integrity in primary cultures of rat brain endothelial cells. *Cell Mol Neurobiol* 2007; 27: 687–694.
28. Zheng L, Ishii Y, Tokunaga A, et al. Neuroprotective effects of PDGF against oxidative stress and the signalling pathway involved. *J Neurosci Res* 2010; 88: 1273–1284.
29. Fleegal MA, Hom S, Borg LK, et al. Activation of PKC modulates blood-brain barrier endothelial cell permeability changes induced by hypoxia and posthypoxic reoxygenation. *Am J Physiol Heart Circ Physiol* 2005; 289: H2012–H2019.
30. Stokum JA, Gerzanich V and Simard JM. Molecular pathophysiology of cerebral edema. *J Cereb Blood Flow Metab* 2016; 36: 513–538.
31. Nikolakopoulou AM, Zhao Z, Montagne A, et al. Regional early and progressive loss of brain pericytes but not vascular smooth muscle cells in adult mice with disrupted platelet-derived growth factor receptor-beta signalling. *PLoS ONE* 2017; 12: e0176225.
32. Villaseñor R, Kuennecke B, Ozmen L, et al. Region-specific permeability of the blood-brain barrier upon pericyte loss. *J Cereb Blood Flow Metab* 2017; 37(12): 3683–3694.
33. Lindahl P, Hellström M, Kalén M, et al. Paracrine PDGFB/PDGF-Rbeta signalling controls mesangial cell development in kidney glomeruli. *Development* 1998; 125: 3313–3322.
34. Nakagawa T, Izumino K, Ishii Y, et al. Roles of PDGF receptor-beta in the structure and function of postnatal kidney glomerulus. *Nephrol Dial Transplant* 2011; 26: 458–468.
35. Hou X, Kumar A, Lee C, et al. PDGF-CC blockade inhibits pathological angiogenesis by acting on multiple cellular and molecular targets. *Proc Natl Acad Sci USA* 2010; 107: 12216–12221.
36. Arimura K, Ago T, Kamouchi M, et al. PDGF receptor beta signalling in pericytes following ischemic brain injury. *Curr Neurovasc Res* 2012; 9: 1–9.
37. Zhang J, Cao R, Zhang Y, et al. Differential roles of PDGFR-alpha and PDGFR-beta in angiogenesis and vessel stability. *FASEB J* 2009; 23: 153–163.
38. Kyyriainen J, Ekolle Ndode-Ekane X and Pitkänen A. Dynamics of PDGFRbeta expression in different cell types after brain injury. *Glia* 2017; 65: 322–341.
39. Al Ahmad A, Gassmann M and Ogunshola OO. Maintaining blood-brain barrier integrity: pericytes perform better than astrocytes during prolonged oxygen deprivation. *J Cell Physiol* 2009; 218: 612–622.
40. Buga AM, Scholz CJ, Kumar S, et al. Identification of new therapeutic targets by genome-wide analysis of gene expression in the ipsilateral cortex of aged rats after stroke. *PLoS One* 2012; 7: e50985.
41. Aguilera KY and Brekken RA. Recruitment and retention: factors that affect pericyte migration. *Cell Mol Life Sci* 2014; 71: 299–309.
42. Nakagomi T, Kubo S, Nakano-Doi A, et al. Brain vascular pericytes following ischemia have multipotential stem cell activity to differentiate into neural and vascular lineage cells. *Stem Cells* 2015; 33: 1962–1974.
43. Sakuma R, Kawahara M, Nakano-Doi A, et al. Brain pericytes serve as microglia-generating multipotent vascular stem cells following ischemic stroke. *J Neuroinflammation* 2016; 13: 57.
44. Yang S, Jin H, Zhu Y, et al. Diverse functions and mechanisms of pericytes in ischemic stroke. *Curr Neuropharmacol* 2017; 15: 892–905.